Direct Methanol Fuel Cell Thermodynamic Simulation

S.S. Sandhu[+,a], R.O. Crowther[a], and J.P. Fellner[b]

[a]Department of Chemical and Materials Engineering, University of Dayton, 300 College Park, Dayton, OH 45469-0246
[b]Air Force Research Laboratory, Propulsion Directorate, Plans and Analysis Branch, 1950 Fifth Street, Wright-Patterson AFB, OH 45433-7251

Abstract

Classical thermodynamics based, mathematical equations are presented for the engineering design/performance analysis of a direct methanol fuel cell (DMFC). The cell model equations account for the presence of chemical species in both liquid and gas phases. Application of the model formulation is illustrated for its steady-state, isothermal operation.

Keywords: Direct methanol fuel cell; Two phase system; Thermal efficiency

[+]Corresponding author: e-mail address: Sarwan.Sandhu@notes.udayton.edu

1. Introduction

The direct methanol fuel cell (DMFC) is considered a viable power production technology for portable electronics equipment (10's-100's watts) and transportation vehicles (10's-100's kilowatts). Since methanol is relatively inexpensive and a reformer or other fuel processing equipment is not required for the DMFC, this power system has the potential to be low cost, compact, reliable and fuel efficient. To supply methanol for the DMFC, only minor modifications to the current gasoline infrastructure would be required. Also, methanol is relatively energy dense compared with hydrogen. Methanol in plastic tanks has a net energy density of 18.9 MJ/kg which is more than twice the 8.3 MJ/kg for hydrogen produced from methanol using a reformer (Larminie and Dicks, 2003).

Figure 1 shows the schematic of an operating DMFC. The DMFC anode consists of a porous carbon-supported platinum-ruthenium catalyst layer backed by a porous carbon/carbon diffusion layer. The cell cathode consists of a porous carbon-supported platinum catalyst layer backed by a carbon/carbon cloth diffusion layer. A proton exchange membrane (PEM), most commonly Nafion^{TM}117, electrically insulates the two electrodes and also serves as the electrolyte. Methanol, in a dilute solution with liquid water, and air are supplied to the DMFC through the anode and cathode channels, respectively, as shown in the sketch. The cell half and overall reactions are given below.

Anode reaction:

$$CH_3OH\,(l) + H_2O\,(l) \Leftrightarrow CO_2\,(g) + 6H^+ + 6e^- \qquad (1)$$

Cathode reaction:

$$1.5\,O_2\,(g) + 6H^+ + 6e^- \Leftrightarrow 3H_2O\,(l) \qquad (2)$$

Overall reaction:

$$CH_3OH\,(l) + 1.5\,O_2\,(g) \Leftrightarrow CO_2(g) + 2\,H_2O\,(l) \tag{3}$$

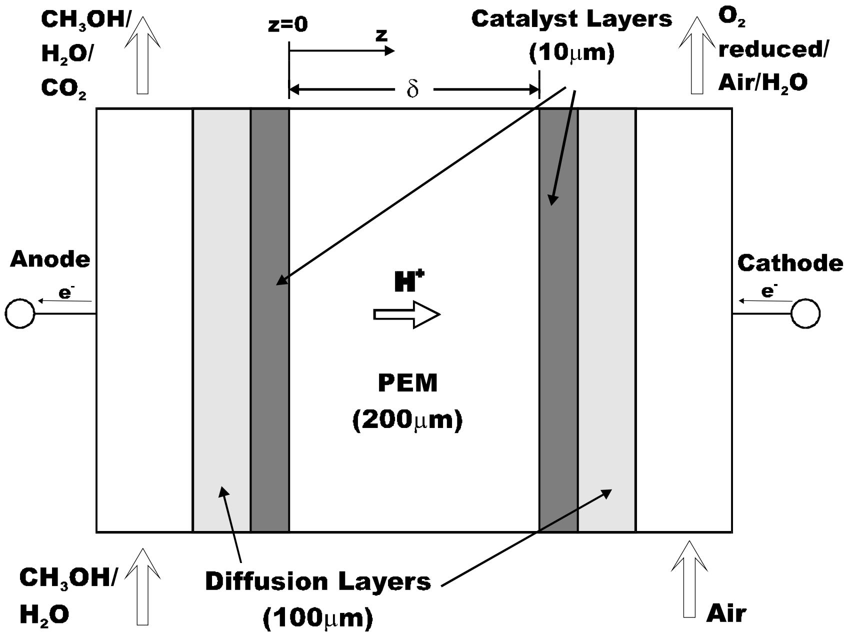

Figure 1. Schematic of an operating direct methanol fuel cell.

Steady-state models and their numerical simulations are necessary to obtain the optimal operating conditions and suggest the potential improvements in a given DMFC (Schultz et al., 2001). Recent modeling activity, based on the chemical engineering science fundamentals, has recently been published (Divisek et al., 2003; Meyers and Newman, 2002; Meyers and Newman, 2002; Meyers and Newman, 2002; Sandhu et al., 2003; Wang and Wang, 2003). From developed species molar balances and the thermodynamic first law, equations to predict the reversible as well as irreversible electric power produced from a continuously fed direct methanol fuel cell operating at steady-state conditions at a given current density were developed. The fuel cell performance equations were numerically simulated by developing a computer code with the cell temperature, pressure, and fuel and oxidant feed stream composition condition as the code input parameters. The developed performance model equations are presented in the next section.

2. Performance model equations

The model equations given in this section are for the steady–state, isothermal operation of a direct methanol fuel cell (DMFC). The equations are here presented on the basis of unit geometric area of an electrode surface perpendicular to the direction of hydrogen ion transport.

2-a. Mole balance equations for chemical species in the cell anode-channel stream:

It is assumed that there is no crossover of carbon dioxide, oxygen, and nitrogen between the cell anode and cathode through the PEM separator. Methanol in liquid water solution enters the cell anode channel. Some of this methanol diffuses to the anode reaction layer for its oxidation with liquid water to produce H^+ ions corresponding to a desired (or fixed) current density i [A/m^2] and some crosses over to the cathode through the PEM separator for its chemical oxidation there. Some of the water entering the anode channel also diffuses to the anode reaction layer for its reaction with methanol and also, some crosses over to the cathode via diffusion/convection and electro-osmotic drag by H^+ ions. The total molar flow rates of methanol, water, and carbon dioxide at the exit of the cell anode channel are given by

$$\dot{n}^A_{CH_3OH} = \dot{n}^A_{CH_3OH,o} - \frac{i}{F}\left(\frac{1}{6} + \zeta_{CH_3OH}\right) \tag{4}$$

$$\dot{n}^A_{H_2O} = \dot{n}^A_{H_2O,o} - \frac{i}{F}\left(\frac{1}{6} + \zeta_{H_2O}\right) \tag{5}$$

$$\dot{n}^A_{CO_2} = \frac{i}{6F} \tag{6}$$

The term $\left(\frac{i}{6F}\right)$ in Eqs. (4), (5), and (6) is indicative of the consumption rates of methanol and water, and production rate of carbon dioxide, respectively, at the anode per unit anode geometric area. $\left(\zeta_{CH_3OH}\right)$ and $\left(\zeta_{H_2O}\right)$ are the moles of methanol and water that crossover to the cathode per mole of H^+ ions that migrate from the anode to cathode reaction layer.

Under the assumption of the anode effluent composed of both liquid and gas/vapor phases in thermodynamic phase equilibrium, modified Raoult's and Henry's laws (Sandhu, 2003; Smith et al., 2001) were used to develop the following equations for iteratively calculating the molar flow rates of methanol, water, and carbon dioxide in both the liquid and vapor phases at the anode exit.

$$\dot{n}^A_{CH_3OH(l)} = \dot{n}^A_{CH_3OH}\left[\frac{\dfrac{P^A}{\gamma^A_{CH_3OH}P^{sat}_{CH_3OH}}}{\dfrac{P^A}{\gamma^A_{CH_3OH}P^{sat}_{CH_3OH}} + \dfrac{\alpha^A}{\beta^A} - 1}\right] \tag{7a}$$

$$\dot{n}^A_{H_2O(l)} = \dot{n}^A_{H_2O}\left[\frac{\dfrac{P^A}{\gamma^A_{H_2O}P^{sat}_{H_2O}}}{\dfrac{P^A}{\gamma^A_{H_2O}P^{sat}_{H_2O}} + \dfrac{\alpha^A}{\beta^A} - 1}\right] \tag{7b}$$

$$\dot{n}^A_{CO_2(d.l.)} = \dot{n}^A_{CO_2}\left[\frac{\dfrac{P^A}{K^A_{CO_2}}}{\dfrac{P^A}{K^A_{CO_2}} + \dfrac{\alpha^A}{\beta^A} - 1}\right] \tag{7c}$$

$$\dot{n}_{CH_3OH(g)} = \dot{n}_{CH_3OH} - \dot{n}_{CH_3OH(l)} \tag{7d}$$

$$\dot{n}_{H_2O(g)} = \dot{n}_{H_2O} - \dot{n}_{H_2O(l)} \tag{7e}$$

$$\dot{n}_{CO_2(g)} = \dot{n}_{CO_2} - \dot{n}_{CO_2(d.l.)} \tag{7f}$$

$$\alpha^A = \dot{n}^A_{CH_3OH} + \dot{n}^A_{H_2O} + \dot{n}^A_{CO_2} \tag{7g}$$

$$\beta^A = \dot{n}^A_{CH_3OH(l)} + \dot{n}^A_{H_2O(l)} + \dot{n}^A_{CO_2(d.l.)} \tag{7h}$$

Where $\dot{n}^A_{i(l)}$ and $\dot{n}^A_{i(g)}$ are the molar flow rates of a chemical species i at the cell anode exit in the liquid and gas phase, respectively; P^A, the anode fuel channel total pressure; P_i^{sat}, the saturated vapor pressure of a chemical species i at the cell temperature; γ_i^A, the activity coefficient of a chemical species i (e.g. CH_3OH, H_2O) in the liquid phase mixture; K_i, the Henry's law constant for a chemical species i (e.g. CO_2).

2-b. Mole balance equations for chemical species in the cell cathode-channel stream:

Humidified air is assumed to enter the cathode channel. Corresponding to the current density, i, per unit geometric area of the cathode reaction layer; oxygen, from air flowing in the cell cathode channel is reduced to produce water in the cathode reaction layer. Also, the crossover methanol is chemically oxidized by oxygen in the cathode reaction layer to produce carbon dioxide and water. Carbon dioxide and water are here assumed to diffuse away, in opposition to the oxygen diffusion direction, from the cathode reaction layer into the cathode channel air stream. The chemical species total mole flow rates at the cathode channel exit are given by

$$\dot{n}^C_{H_2O} = \dot{n}^C_{H_2O,o} + \frac{i}{F}\left(0.5 + 2\zeta_{CH_3OH} + \zeta_{H_2O}\right) \tag{8a}$$

$$\dot{n}^C_{CO_2} = \frac{i\zeta_{CH_3OH}}{F} \tag{8b}$$

$$\dot{n}^C_{O_2} = \dot{n}^C_{O_2} - \frac{i}{F}\left(0.25 + 1.5\zeta_{CH_3OH}\right) \tag{8c}$$

$$\dot{n}^C_{N_2} = \dot{n}^C_{N_2,o} = 3.76\dot{n}^C_{O_2,o} \qquad \text{(8d)}$$

From the thermodynamic view point, if the mole fraction of water at the cathode exit is less than its mole fraction when the gas phase is saturated with water at the prevailing temperature and pressure conditions, one may neglect presence of very small amount of liquid water in tiny droplets, if any, and consider the entire cathode channel stream leaving the cell in the gas phase. Mathematically, this statement may also be represented as:

$$\frac{z^C_{H_2O}}{1-z^C_{H_2O}} < \frac{\dfrac{P^{sat}_{H_2O}}{P^C}}{1-\dfrac{P^{sat}_{H_2O}}{P^C}} \qquad \text{(9)}$$

$$\begin{pmatrix}\text{actual moles of water in the gas}\\ \text{phase per mole of gas mixture}\\ \text{excluding water vapor}\end{pmatrix} < \begin{pmatrix}\text{moles of water in the gas phase saturated}\\ \text{with water vapor per mole of gas}\\ \text{mixture excluding water}\end{pmatrix}$$

where $z^C_{H_2O}$ = mole fraction of water vapor in the gas phase at the exit of the cell cathode channel. If the above inequality is not satisfied, both liquid and vapor phases are likely to coexist at the cathode channel exit.

2-c. Thermodynamic first-law based equations

The actual power density, $\dot{W}_{irr}$, of a direct methanol fuel cell (DMFC) can be calculated from the following form of the first law of classical thermodynamics for given cell current density, temperature, pressure, and channel feed flow rate composition conditions.

$$\dot{W}_{irr} = \begin{bmatrix} \sum_j \dot{n}^A_{j(l)}\overline{H}^A_{j(l)} + \sum_j \dot{n}^A_{j(g)}\overline{H}^A_{j(g)} - \sum_j \dot{n}^A_{j,o}\overline{H}^A_{j,o} + \\ \sum_j \dot{n}^C_{j(l)}\overline{H}^C_{j(l)} + \sum_j \dot{n}^C_{j(g)}\overline{H}^C_{j(g)} - \sum_j \dot{n}^C_{j,o}\overline{H}^C_{j,o} \end{bmatrix} - \frac{\dot{Q}}{A} \qquad \text{(10)}$$

where, $\dot{n}^A_j, \dot{n}^C_j$ are the molar flow rate of a chemical species j in the phase indicated by the subscript in the cell anode and cathode flow channel, respectively, based on unit geometric area of a cell electrode; $\overline{H}^A_j, \overline{H}^C_j$ are the partial molar enthalpy of a chemical species j in the anode and cathode channel stream, respectively. In Eq. (10), subscripts $l, g, \circ$ represent the liquid phase, gas phase, and feed, respectively. $\frac{\dot{Q}}{A}$ is the heat-exchange rate per unit cell electrode geometric area between the cell and its environment. The total heat exchange rate, $\dot{Q}$, is positive if heat is added to the DMFC system, negative if it is lost from the system. “A” is the cell total electrode geometric area.

One can obtain the cell voltage of an operating DMFC to deliver the cell "useful", external circuit electric current density, i, from the following equation:

$$E_{irr} = \frac{\left|\dot{W}_{irr}\right|}{i} \tag{11}$$

The magnitude of the irreversible power density, $\left|\dot{W}_{irr}\right|$, for its use in Eq. (11) is provided by Eq. (10).

The thermal efficiency of a DMFC is here defined as the ratio of the actual power density to the total thermal energy that corresponds to a desired level of the external circuit current density. This is the efficiency that is used to compare the performance of a DMFC with that of a heat engine. The DMFC thermal efficiency can be computed from the following equation.

$$\eta_{thermal} = \frac{\begin{bmatrix} \sum_j \dot{n}^A_{j(l)} \overline{H}^A_{j(l)} + \sum_j \dot{n}^A_{j(g)} \overline{H}^A_{j(g)} - \sum_j \dot{n}^A_{j,o} \overline{H}^A_{j,o} + \\ \sum_j \dot{n}^C_{j(l)} \overline{H}^C_{j(l)} + \sum_j \dot{n}^C_{j(g)} \overline{H}^C_{j(g)} - \sum_j \dot{n}^C_{j,o} \overline{H}^C_{j,o} \end{bmatrix} - \frac{\dot{Q}}{A}}{\begin{bmatrix} \sum_j \dot{n}^A_{j(l)} \overline{H}^A_{j(l)} + \sum_j \dot{n}^A_{j(g)} \overline{H}^A_{j(g)} - \sum_j \dot{n}^A_{j,o} \overline{H}^A_{j,o} + \\ \sum_j \dot{n}^C_{j(l)} \overline{H}^C_{j(l)} + \sum_j \dot{n}^C_{j(g)} \overline{H}^C_{j(g)} - \sum_j \dot{n}^C_{j,o} \overline{H}^C_{j,o} \end{bmatrix}} \tag{12}$$

3. Application of the developed/assembled thermodynamic DMFC performance simulation

A computer program was developed in Microsoft Visual Basic 6.0 (Crowther, 2003) to generate numerical data from the model DMFC performance equations. The input parameters to the computer code are: cell current density, cell temperature, anode and cathode flow channel pressures, anode channel fuel stream methanol concentration and volumetric flow rate, cathode channel air stream volumetric feed rate and its relative humidity, channel inlet feed temperature and pressure conditions if different from the cell temperature and pressure conditions, electrode geometric area, and cell heat-loss per unit electrode geometric area. Note that Eq. (10) can either be used to predict the power generated from a DMFC if the heat-loss, $\frac{\dot{Q}}{A}$, data is available or $\frac{\dot{Q}}{A}$ can be predicted if the actual power produced, $\dot{W}_{irr}$, is known.

Application of the developed DMFC performance simulation is illustrated by the plots generated from the limited numerical data as shown in Figures 2 and 3. The data presented in these figures correspond to the methanol solution feed rate of 5 ml/min and the cell electrode geometric cell area of 5 cm^2. For anode and cathode pressures of 1 bar, heat loss per unit electrode area was estimated for the current density of 1000 A/m^2 at the desired temperature of 80^{o}C using published data (Gurau and Smotkin, 2002). Also, ζ_{CH_3OH} and ζ_{H_2O} were estimated (Crowther, 2003) using the experimental data (Ren et al., 1995). Figure 2 shows the predicted actual cell voltage versus methanol feed concentration at 80^{o}C. A slight increase in the predicted cell voltage, for methanol concentrations greater than 750 g-mol/m^3, may be mainly due to some inaccuracy involved in the estimation of the methanol crossover coefficient and heat loss from the experimental data. Figure 3 shows the predicted actual thermal efficiency as a function of methanol feed concentration at the cell temperature of 353.15 K and current density of 1000 A/m^2. Thermal efficiency decreases as the methanol concentration in the anode channel feed increases due to the fact that at higher methanol concentrations, the methanol crossover flux is higher. Thus, at higher methanol concentrations, relatively more heat has to be removed from the cell for steady-state operation.

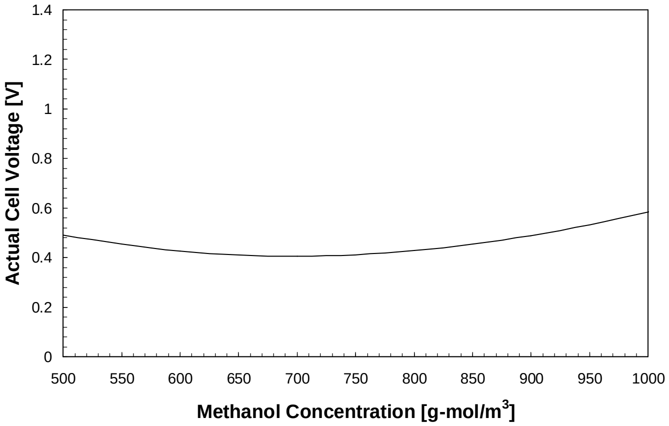

Figure 2. Actual cell irreversible voltage as a function of methanol feed concentration at 80 ^{o}C and a current density of 1000 A/m^2.

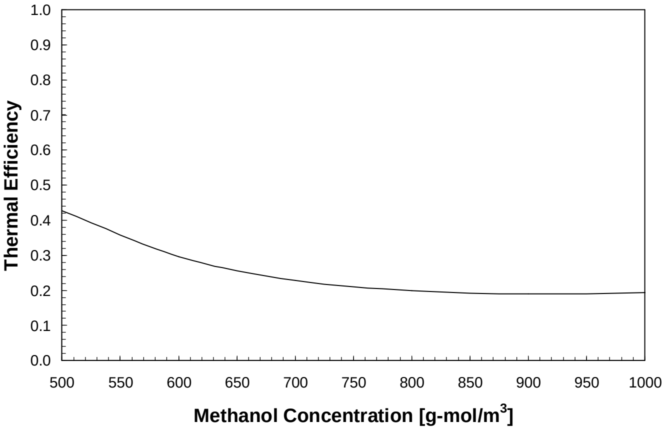

Figure 3. DMFC efficiency as a function of methanol feed concentration at a temperature of 353.15K and a current density of 1000 A/m^2.

4. Concluding remarks

A general model, based on classical thermodynamics, has been presented for analyzing the performance or for designing a DMFC. Application of the model has been illustrated by generating numerical data from a computer program that was specifically developed to numerically simulate the model equations. To further improve the modeling capability to predict DMFC performance, a rigorous model equation for the cell heat loss, based on theoretical/experimental data, should be developed. The presented model, coupled with the new heat loss equation, should then be verified with experimental data from a DMFC for its validation over a wider range of temperature, pressure, and reactant feed compositions. Also, development of a general equation to calculate ζ_{CH_3OH} as a function of current density, methanol concentration, and temperature is needed. The classical thermodynamics based approach presented here can be further extended for the performance prediction/design of other fuel cells such as hydrogen/air PEM fuel cells, phosphoric acid electrolyte fuel cells (PAFC), and solid oxide fuel cells (SOFC).

Acknowledgement

Financial support for this work was provided, in part, by the Dayton Area Graduate Studies Institute (R.O.Crowther) and the Air Force Research Laboratory, Wright-Patterson AFB,Ohio under contract no. F33615-98-D-2891, Delivery Order 17.

References

Crowther RO. Partial numerical simulation of direct methanol fuel cell performance. Dayton: University of Dayton; 2003.

Divisek J, Fuhrmann J, Gartner K, Jung R. Performance Modeling of a Direct Methanol Fuel Cell. J Electrochem Soc 2003; 150 (6):A811-A825.

Gurau B, Smotkin ES. Methanol crossover in direct methanol fuel cells: a link between power and energy density. J Power Sources 2002; 112:339-352.

Larminie J, Dicks A. Fuel Cell Systems Explained. (2nd edition). West Sussex: Wiley, 2003.

Meyers JP, Newman J. Simulation of the Direct Methanol Fuel Cell I. Thermodynamic Framework for a Multicomponent Membrane. J Electrochem Soc 2002; 149 (6):A710-A717.

Meyers JP, Newman J. Simulation of the Direct Methanol Fuel Cell II. Modeling and Data Analysis of Transport and Kinetic Phenomena. J Electrochem Soc 2002; 149 (6):A718-A728.

Meyers JP, Newman J. Simulation of the Direct Methanol Fuel Cell III. Design and Optimization. J Electrochem Soc 2002; 149 (6):A729-A735.

Ren X, Zawodzinski TA, Uribe F, Hongli D, Gottesfeld S. Methanol cross-over in direct methanol fuel cells. In First International Symposium on Proton Conducting Membrane Fuel Cells. Chicago, IL: Electrochem. Soc, Pennington, NJ, USA; 1995. 284-298 p.

Sandhu SS. Unpublished technical notes. Dayton: University of Dayton, 2003.

Sandhu SS, Crowther RO, Krishnan SC, Fellner JP. Direct methanol polymer electrolyte fuel cell modeling: reversible open-circuit voltage and species flux equations. Electrochim Acta 2003; 48:2295-2303.

Schultz T, Zhou S, Sundmacher K. Current status of and recent developments in the direct methanol fuel cell. Chem Eng Technol 2001; 24 (12):1223-1233.

Smith JM, Ness HCV, Abbott MM. Introduction to chemical engineering thermodynamics. (6th edition). Boston: McGraw-Hill, 2001.

Wang ZH, Wang CY. Mathematical Modeling of Liquid-Feed Direct Methanol Fuel Cells. J Electrochem Soc 2003; 150 (4):A508-A519.